

# Supporting Information

## Asymmetric phosphorus incorporation in homoepitaxial P-doped (111) diamond revealed by photoelectron holography

*T. Yokoya,<sup>\*,†,‡</sup> K. Terashima,<sup>†,#</sup> A. Takeda,<sup>‡</sup> T. Fukura,<sup>‡</sup> H. Fujiwara,<sup>‡</sup> T. Muro,<sup>||</sup> T. Kinoshita,<sup>||</sup> H. Kato,<sup>§</sup> S. Yamasaki,<sup>§</sup> T. Oguchi,<sup>#</sup> T. Wakita,<sup>†</sup> Y. Muraoka,<sup>†,‡</sup> and T. Matsushita<sup>\*,||</sup>*

<sup>†</sup>Research Institute for Interdisciplinary Science (RIIS), Okayama University, Okayama 700-3537, Japan

<sup>‡</sup>Graduate School of Science and Technology, Okayama University, Okayama 700-3537, Japan

<sup>||</sup>Japan Synchrotron Radiation Research Institute (JASRI)/SPring-8, 1-1-1 Kouto, Sayo, Hyogo 679-5198, Japan

<sup>§</sup>Energy Technology Research Institute, National Institute of Advanced Industrial Science and Technology (AIST), Tsukuba Center 2, Tsukuba, Ibaraki 305-8568, Japan

<sup>#</sup>Institute of Scientific and Industrial Research, Osaka University, 8-1 Mihogaoka, Ibaraki, Osaka 567-0047, Japan

\*e-mail: T. Y. (yokoya@cc.okayama-u.ac.jp), T. M. (matusita@spring-8.or.jp)

# I. Simulated photoelectron holograms for substitutional P, PVSVC, and interstitial P

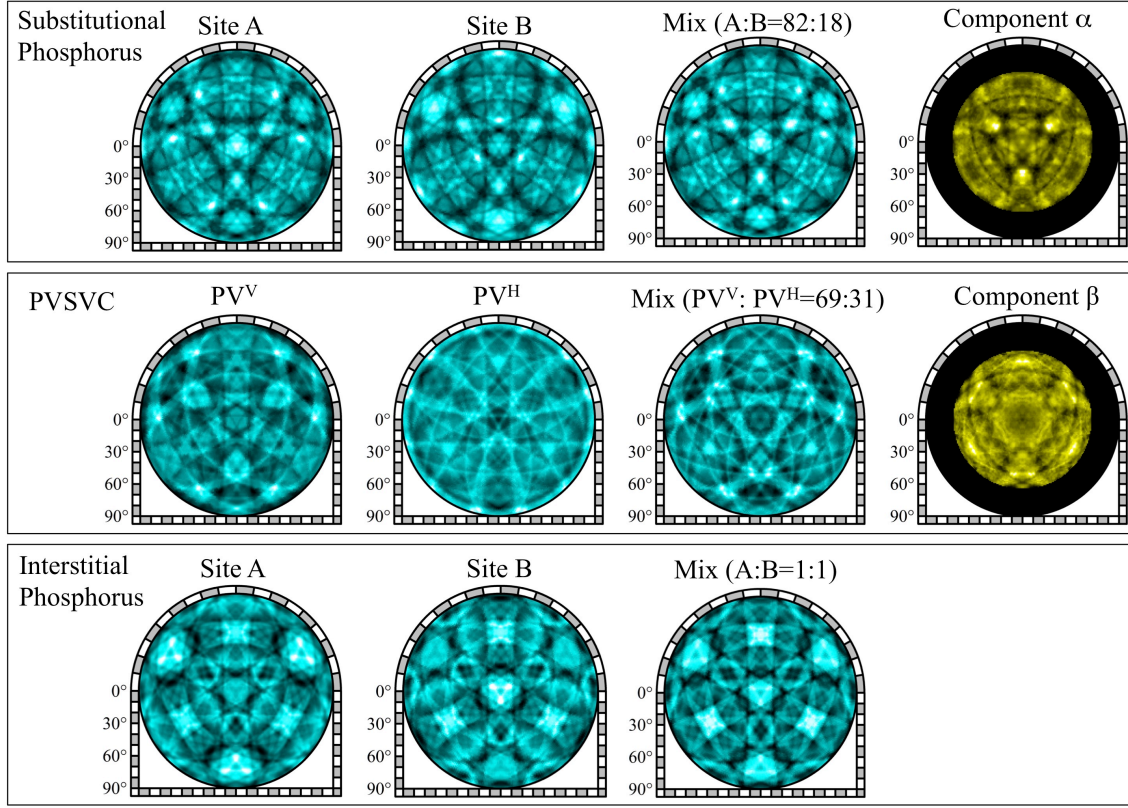


**Figure S1.** Comparison of experimental and simulated holograms

Simulated photoelectron holograms (sky blue) for substitutional P, PV split-vacancy complex(PVSVC), and interstitial P, together with the experimental photoelectron holograms of components  $\alpha$  and  $\beta$  of P 2p core level (yellow) are presented herein. The occupancy ratios of the A and B sites for substitutional P and Interstitial P as well as that of the  $PV^V$  and  $PV^H$  for PVSVC was calculated by a fitting method. The mean square error function  $F$  used in the fitting calculation is defined as

$$F = \|aI^A + bI^B + c - I^E\|^2,$$

where  $I^A$ ,  $I^B$ , and  $I^E$  are the images of the simulated holograms of the A and B sites, and the hologram obtained by the experiment, respectively. The parameters  $a$ ,  $b$ , and  $c$  can be obtained by minimizing  $F$ , and the ratio of the A and B sites is given by the parameters  $a$  and  $b$ .

For PVSVC,  $I^A$  and  $I^B$  are the images of the simulated holograms of  $PV^V$  and  $PV^H$  ( $= PV^{H1} + PV^{H2} + PV^{H3}$ ), respectively, where geometrically expected relative ratio is  $PV^V:PV^H=50:50$

## II. Details of PEH technique

There are mainly two types of PEH equipment that are used frequently these days. One is a two-dimensional display-type analyser, where an angular distribution of the azimuthal angle ( $\phi$ ) of  $2\pi$  and the polar angle ( $\theta$ ) of  $\pm 60^\circ$  [H. Daimon, Rev. Sci. Instrum. 59, 545 (1988).] and  $\pm 45^\circ$  [T. Muro, Rev. Sci. Instrum. 88, 123106 (2017).] can be obtained at a time. The other is the combination of an angle-resolved electron energy analyser and a sample manipulation that can sweep  $\theta$  and  $\phi$  of the sample with respect to the analyser. This type of measurement system has an advantage of high energy resolution but takes more time to obtain a photoelectron hologram. In the present study, the PEH measurement was performed with a Scienta Omicron DA30 hemispherical analyser, which enables us to measure energy distribution of photoelectrons with a wide acceptance angle (maximum  $\pm 10^\circ \times \pm 15^\circ$ ) without changing the angles by virtue of the deflector lens of the DA30 (Fig. S2). The spatial resolution estimated using a scattering pattern function is  $\sim 0.030$  nm for photoelectron kinetic energy of 500 eV, which increases (decreases) for higher (lower) kinetic energy [T. Matsushita et al., J. Electron Spectrosc. Relat. Phenom. 178–179, 195 (2010)]. For this study, we selected the angular region of  $\pm 6^\circ \times \pm 10^\circ$  and set the angular resolution of  $0.5^\circ$ . To map out the angular distribution of core-level photoelectron intensity for a wider angular region for obtaining a hologram, a series of measurements was performed by changing  $\theta$  ( $0^\circ, 9^\circ, 18^\circ, 27^\circ, 36^\circ, 45^\circ, 54^\circ$ , and  $63^\circ$ ) and  $\phi$  ( $0^\circ, 15^\circ, 30^\circ, 45^\circ$ , and  $60^\circ$ ). The energy resolution needed to resolve different chemical components was set to  $\sim 170$  meV.

A sample was irradiated with synchrotron light incident at a grazing angle of  $5^\circ$  with respect to the sample surface. The spot size on the sample surface was  $\sim 150 \times 50 \mu\text{m}^2$ . In this grazing incidence, the light penetrates the diamond sample up to a depth of 60 nm, and the electrons involved in the core-level photoemission signals only come from the depth of the order of 1 nm, as expected from the mean free path of the photoelectrons. Therefore, in this volume there are  $1 \times 10^{12}$  of carbon atoms and  $8 \times 10^8$  of phosphorous atoms.

PEH has the following features. The scattered wave is mainly formed by core potentials, such that the effect of the density modulation of the valence, such as surface state, is negligible. In addition, effect of the surface roughness, surface step, and defects (including etch pits) independent on the dopant are also negligible, because the

measured hologram is the sum of all the dopants in the light spot area such that the dominant structures of the dopants is enhanced. Therefore, the defects linking to the dopant are observable, as shown herein. Lattice distortion expected at a higher doping range can be observed (not as a mean lattice distortion that can be observed from x-ray diffraction but as a local lattice distortion around a dopant) with PEH in principle if the distortion is large enough to detect.

Regarding requirements for PEH, minimum thickness of a sample should be of the order of the mean free path of photoelectrons. To perform PEH experiments within a reasonable machine time of 3–4 days, a sample with a doping concentration of  $1 \times 10^{20} \text{ cm}^{-3}$  may be necessary. Importantly, a sample is conductive for preventing charging, which alters the binding energy and even the spectral shape of a core-level spectrum. Therefore, we do not measure the insulating intrinsic diamond. It is better to use a conductive substrate to be supplied with electrons.

The intensity of the reconstructed 3D atomic image is related to the probability of existence of an atom, not electron density, because the photoelectron is mainly scattered by the Coulomb potential of atomic nucleus shielded outside with core electrons and valence electrons. When the experimentally obtained hologram is perfectly normalized, the intensity becomes the probability of existence of an atom; however, its estimation is difficult because of photoelectron background, etc. When the normalization of hologram is imperfect, the entire atomic image intensity is changed but the atomic position and relative atomic image intensities remain unchanged. Therefore, the unit becomes arbitrary unit.

Even if atomic distribution function is treated as the probability of existence of an atom, an atomic image usually shows a special shape because of the inverse transformation of the algorithm. This discussion was carried out in references 3 and 4.

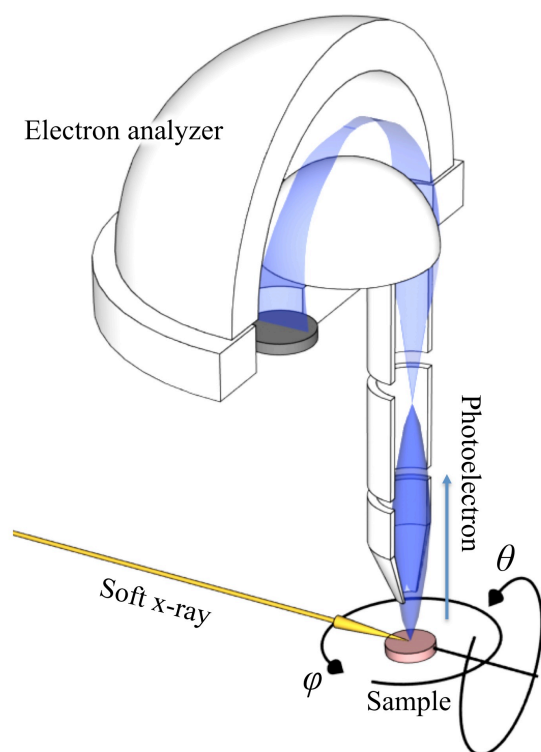


**Fig. S2.** Experimental set up for PEH measurements.

#### References

- (1) Daimon, H. New display-type analyzer for the energy and the angular distribution of charged particles. *Rev. Sci. Instrum.* **1988**, 59, 545–549.
- (2) Muro, T.; Ohkouchi, T.; Kato, Y.; Izumi, Y.; Fukami, S.; Fujiwara, H.; Matsushita, T. Wide-angle display-type retarding field analyzer with high energy and angular resolutions, *Rev. Sci. Instrum.* **2017**, 88, 123106.
- (3) Matsushita, T.; Matsui, F.; Daimon, H.; Hayashi, K. Photoelectron holography with improved image reconstruction. *J. Electron Spectrosc. Relat. Phenom.* **2010**, 178–179, 195–220.
- (4) Matsushita, T.; Agui, A.; Yoshigoe, A. A new approach for three-dimensional atomic-image reconstruction from a single-energy photoelectron hologram. *Europhys. Lett.*, **2004**, 65, 207–213.